Generalized Generic Model Control of High-purity Internal Thermally Coupled Distillation Column Based on Nonlinear Wave Theory

Lin Cong, Xinggao Liu, Yexiang Zhou, and Youxian Sun
State Key Laboratory of Industrial Control Technology, Control Department, Zhejiang University, Hangzhou 310027, P.R. China

DOI 10.1002/aic.14141
Published online June 21, 2013 in Wiley Online Library (wileyonlinelibrary.com)

A new model-based control strategy for the internal thermally coupled distillation column (ITCDIC) is presented. Based on the nonlinear wave theory that describes the nonlinear dynamics in the separation processes, a simplified nonlinear wave model is established that concerns both the wave propagation and the profile shape. An advanced controller (WGGMC) is formulated by combining the nonlinear wave model with a generalized generic model control (GGMC). Compared with a conventional generic model controller based on a data-driven model (TGMC), and another wave-model based generic model controller (WGMC) developed in our previous work, WGGMC exhibits the best performances in both servo control and regulatory control. Furthermore, WGGMC can handle a very-high-purity system of ITCDIC with top product composition of 0.99999, while the other two controllers fail to work. © 2013 American Institute of Chemical Engineers *AIChE J*, 59: 4133–4141, 2013

Keywords: Internal thermally coupled distillation column, very high purity, simplified nonlinear wave model, generalized generic model control

Introduction

Distillation is one of the most widely used unit operations in chemical industry. However, the high-energy consumption and relatively low-energy efficiency of distillation make a large amount of energy wasted. Any improvement of the energy efficiency in distillation will economize a great deal of energy.[1–4] The internal thermally coupled distillation column (ITCDIC) is a new kind of column in which internal thermally coupling is adopted between the rectifying section and the stripping section. For a conventional distillation column, an additional heat source has to be introduced in the reboiler and the hot flow is cooled down in the condenser, and, therefore, a great deal of energy is wasted. However, ITCDIC has neither a reboiler nor a condenser during normal operation, and heat exchange is accomplished between the rectifying section and the stripping section, which is shown in Figure 1. So the energy efficiency is largely improved. In order to provide the necessary thermal driving force for the heat transfer, the rectifying section is operated at a higher pressure than the stripping section.[5–12] Recently, a work by Cabrera-Ruiz et al.[13] has shown that when one includes the compressing energy the savings are significantly affected, and in some cases hybrid structures which combine HIDiC (heat-integrated distillation column) and conventional columns have been proved to have higher economic potential than that totally using HIDiC in the separation of ternary mixtures, which reveals that the use of HIDiC should be carefully investigated for certain mixtures before real applications.

Because of the high degree of thermal coupling relations between the two sections of ITCDIC, the interactions are highly intensified as manifested in the following aspects: high nonlinearity, asymmetric behavior, inverse response and high sensitivity to external disturbances. The complex dynamics bring a lot of trouble in modeling and control design.[2,8,14–20] The great majority of modeling is based on linear approximation or data for simplicity. Most controllers of ITCDIC are also based on the linear approximation model or the data-driven model. PID, and IMC using reduced-order model are proposed by Naikawa and Zhu et al.[15,21–23] Recently, an adaptive GMC and an adaptive GPC are also researched by Liu et al.[24,25] These control strategies can work well in the neighborhood of the nominal operating point for set-point transfer and external disturbances. However, when the operating conditions have a sharp change, most of the controller's performances deteriorate obviously, because the large model mismatch between the simplified model and the real plant destroys the robustness of the controller. Especially when the concentration of the column end reaches an extremely high purity, the model mismatch is more pronounced and the tight control of the dual-end cannot be realized by these linear approximation model and data-driven model. Although first-principle model[7] is an effective model to capture the dynamics of ITCDIC, its complex structure makes it hardly used in a control model. In

Correspondence concerning this article should be addressed to X. Liu at lxg@zju.edu.cn.

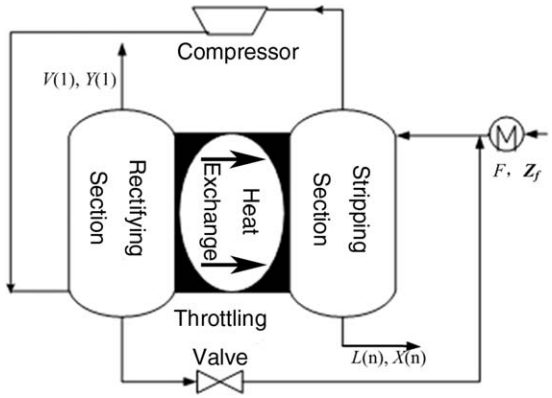

Figure 1. Schematic diagram of an ideal ITCDIC.

consideration of the aforementioned fact, an advanced nonlinear model must be established for more effective controllers, which should contain the following characteristics: accurately describing the dynamics of ITCDIC and the structure simple enough for control design.[26]

Early research on chromatography proposed a wave theory to describe the distinct behavior in the separation processes. Systems with distributed parameters often exhibit dynamic phenomena which resemble traveling waves.[27–29] This theory has been successfully extended to conventional distillation columns.[30,31] Hwang established a nonlinear wave theory for conventional binary distillation columns.[32,33] The theory clearly presented the dynamic behavior of distillation columns such as high steady-state gains, large response lags, strong nonlinearity and asymmetric dynamics and a wave velocity was derived to describe the movement of the wave profile. From then on, the wave theory is widely used in modeling of distillation columns and control design. Marquardt drew on the wave theory to characterizing the distillation column dynamics and proposed rigorous wave velocity formula and the function of the wave profile from differential material balances.[34] Kienle used wave theory for modeling in ideal multicomponent distillation processes.[35] Balasubramhanya[36] developed a low-order wave model for high-purity distillation columns with online updated profile parameters. Luyben[37,38] pioneered a study of profile propagation and profile position control in high-purity distillation columns. Based on the wave model, a novel generic model control strategy was proposed to control a traditional distillation column by Han and Park.[39] Group led by Henson introduced a model predictive control based on wave model in nitrogen purification columns.[40–42] An extension of the wave model to variable flow rates in a conventional distillation column was presented by Stein et al.[43] Also, Hankins[44] developed a wave model with varied molar flow rates and demonstrated that the assumption of constant pattern wave still held true in conventional distillation columns. As will become apparent from the literature reviewed, wave theory is a promising tool to characterize the dynamics of distillation columns. However, since the construction of ITCDIC is quite different from that of a conventional distillation column, the nonlinear wave theory cannot be directly applied to the modeling of ITCDIC, because molar flow rates in ITCDIC change drastically over every stage due to the internal thermally coupling.[45] Liquid mole flow is cumulated from the top stage to the bottom, and vapor mole flow is cumulated from the bottom stage to the top. Also the shape of wave changes more obviously than that in a conventional distillation column, which makes the wave velocity computation more difficult. In our previous work,[46] a nonlinear wave model of ITCDIC was proposed and a generic model control strategy for ITCDIC based on the proposed model was designed, however, compositions in each tray should be measured for the estimation of wave velocity and there were many differential terms in the wave model, so some errors in the variables to be differentiated might lead to amplification of the error and hence a more simplified wave model is required.

In this work, a simplified nonlinear wave model is established for ITCDIC. The wave velocity is first derived from the profile function and differential material balances in ITCDIC, and then a nonlinear wave model of ITCDIC is established. Based on the proposed wave model, a generalized generic model controller (WGGMC) is developed for ITCDIC. In the case study, another two GMC controllers, which are based on a data-driven model (TGMC) and a nonlinear wave model (WGMC) presented by Liu et al.[6] respectively, are adopted for comparison. Results prove the efficiency of the proposed nonlinear wave model of ITCDIC, and WGGMC shows its excellent performance in servo control and regulatory control. Especially, WGGMC realizes the very high-purity control with the top product composition of 99.999%, whereas the other controllers fail to work properly.

Simplified Nonlinear Wave Model of ITCDIC

Dynamics of separation processes could be described by the propagation of concentration profile. In distillation columns, nonlinear wave can be imagined as a spatial structure (concentration profile) moving with a certain propagation velocity along a spatial coordinate. Therefore, two factors are essential for building the nonlinear wave model: the describing function of concentration profile and the derivation of the wave velocity.

In conventional distillation columns, the profile shape is analytically derived by Marquardt under a second-order polynomial approximation to vapor–liquid equilibrium. In ITCDIC, the same method is used and the profile function is derived[46]

$$\hat{X}(j)=X_{r\_\min}+\frac{X_{r\_\max}-X_{r\_\min}}{1+\exp\left(-k_r(j-S_1)\right)},\qquad j=1,2,...,f-1 \tag{1}$$

$$\hat{X}(j)=X_{s\_\min}+\frac{X_{s\_\max}-X_{s\_\min}}{1+\exp\left(-k_s(j-S_2)\right)},\qquad j=f,f+1,...,n \tag{2}$$

where $X_{r\_\max}$, $X_{r\_\min}$, k_r, $X_{s\_\max}$, $X_{s\_\min}$, k_s are the six profile parameters which are generated from the composition concentration data calculated from the mechanism model of ITCDIC[7]. $X_{r\_\min}$ and $X_{r\_\max}$ denote the asymptotic limits of the rectifying section when the profile extends to an infinite distance; $X_{s\_\min}$ and $X_{s\_\max}$ denote the asymptotic limits in the stripping section. k_r,k_s characterize the tangent of the inflection points S_1 and S_2 (k_r, k_s do not equal the tangents). S_1 and S_2 are the representations of the profile positions in the rectifying section and stripping section, respectively. Nonlinear least-square estimation is employed to calculate the initial values of the six parameters and update them online (take rectifying section as an example)

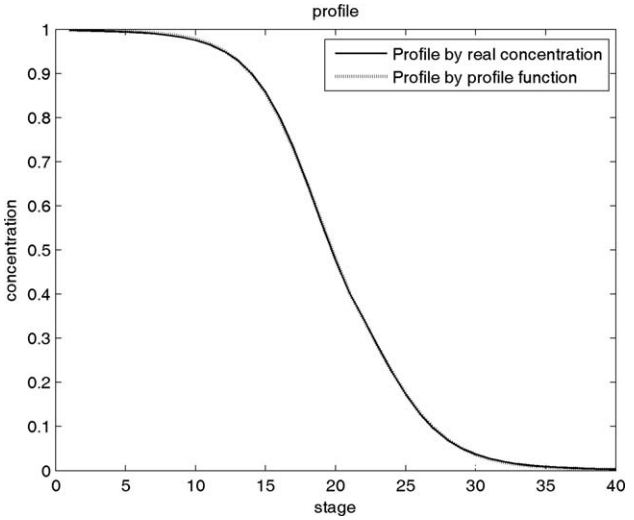

Figure 2. The liquid concentration by the profile function and real concentration at the initial steady state.

$$\begin{aligned} \min \quad & \sum_{i=1}^{f-1}\left(\hat{X}_j - X_j\right)^2 \\ \text{st.} \quad & \hat{X}_1 - X_1 = 0 \\ & \hat{X}_{f-1} - X_{f-1} = 0 \\ & X_{r\_\min} - X_{r\_\max} < 0 \\ & 0 < Xr\_\max < 1 \\ & 0 < Xr\_\min < 1 \end{aligned}$$

In this work, benzene-toluene system is taken as an illustration. Figure 2 shows the concentration profiles by real concentration of the initial steady state and by the profile function, respectively when the column works in the stable operating point. The operating conditions are listed in Table 1. From Figure 2, we can see that the two curves almost coincide with each other. Therefore, in order to distinguish the two profiles clearly, the differences between the two profiles are given in Figure 3. The result shows that the two profiles are very close to each other and the largest deviation is less than 0.003, which confirms the validity of the profile function.

In the previous work,[46] we derived the wave velocity by cumulatively integrating the relationships between wave velocity and the material balances in each column stage. From Figure 3, we have already known that the errors are oscillating around zero, but the amplitude and the frequency are irregular, so the cumulative integration of all stages might increase the error. As shown in Figure 3, the errors near the top and bottom of the column (stage 1 and stage n) are almost equal to zero, which means that the profile function has higher accuracy at the two ends of the column. If we derive the wave velocity from stages 1 and n, not cumulative integration of all stages, the errors of stages 1 and n between the real concentration obtained from the mechanism model[7] and the concentration from the wave model could be further eliminated. Based on the aforementioned consideration, the simplified nonlinear wave model is proposed.

The component mass balances in stages 1 and n of ITCDIC are as follows

$$HdX_1/dt = V_2Y_2 - V_1Y_1 - L_1X_1 \tag{3}$$

$$HdX_n/dt = -V_nY_n + L_{n-1}X_{n-1} - L_nX_n \tag{4}$$

In Eqs. 1 and 2, the parameters such as $X_{r\_\max}$, $X_{r\_\min}$, k_r, $X_{s\_\max}$, $X_{s\_\min}$ and k_s change little with variation of time, so we give the assumption that the parameters mentioned previously have no time dependence and the derivatives of them are approximate to zero. Combining Eq. 1 when $j = 1$, Eq. 2 when $j = n$, with Eqs. 3 and 4, we can obtain the wave velocity by derivation of Eqs. 1 and 2 on both sides

$$\frac{dS_1}{dt} = \frac{(1+\exp(-k_r(1-S_1)))^2(V_2Y_2 - V_1Y_1 - L_1X_1)}{-k_rH(X_{r\_\max} - X_{r\_\min})\exp(-k_r(1-S_1))} \tag{5}$$

$$\frac{dS_2}{dt} = \frac{(1+\exp(-k_s(n-S_2)))^2(-V_nY_n + L_{n-1}X_{n-1} - L_nX_n)}{-k_sH(X_{s\_\max} - X_{s\_\min})\exp(-k_s(n-S_2))} \tag{6}$$

Combining Eqs. 1, 2, 5 and 6 with thermally coupled relations, vapor and liquid molar flow rates and vapor–liquid equilibrium relationships, we can establish the simplified nonlinear wave model of ITCDIC. The other relations are listed as follows:

Thermally coupled relations

$$Q_j = UA\left(T_j - T_{j+f-1}\right), (j=1,\ldots,f-1) \tag{7}$$

$$T_j = b/\left(a - \ln p_{vp,j}\right) - c \tag{8}$$

$$P_{vp,j} = P/\left[X_j + \left(1-X_j\right)/\alpha\right] \tag{9}$$

Vapor and liquid molar flow rates

$$L_1 = Q_1/\lambda \tag{10}$$

$$L_{n-1} = \sum_{k=1}^{f-1} Q_k/\lambda + Fq - \sum_{k=1}^{f-2} Q_k/\lambda \tag{11}$$

$$V_1 = F(1-q) \tag{12}$$

$$L_n = F - V_1 \tag{13}$$

$$V_2 = V_1 + L_1 \tag{14}$$

$$V_n = V_1 + \sum_{k=1}^{f-1} Q_k/\lambda - F(1-q) - \sum_{k=1}^{f-2} Q_k/\lambda \tag{15}$$

Vapor–liquid equilibrium relationships

Table 1. Operating Conditions

Name	Value	Name	Value
Stage number	40	Feed thermal condition	0.501
Feed stage	21	Pressure of stripping section[MPa]	0.3387
Feed flow rate [kmol/h]	100	Heat transfer rate in each stage[W/K]	9803
Feed composition (benzene)	0.5	Latent heat of vaporization[kJ/kmol]	30001.1
(toluene)	0.5	Liquid holdup in each stage[kmol]	1.5
Relative volatility (α)	2.317	Antoine constant (a)	15.9008
Antoine constant (b)	2788.51	Antoine constant (c)	−52.36

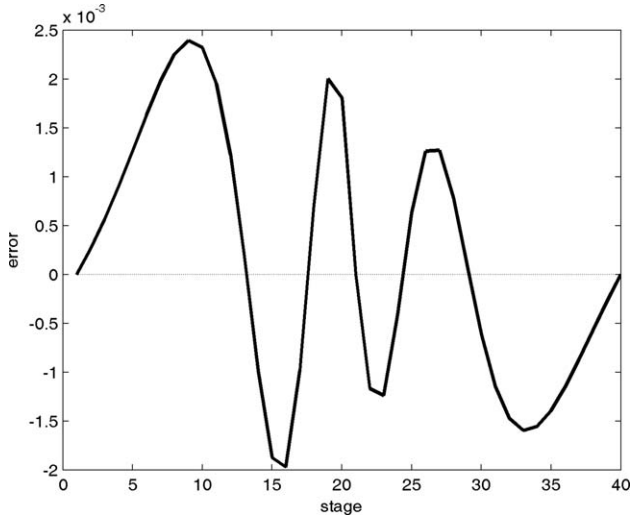

Figure 3. The errors between the profile function and real concentration at the initial steady state.

$$Y_j=\alpha X_j/\left[(\alpha-1)X_j+1\right],(j=1,2,n) \tag{16}$$

According to Eqs. 8 and 9, the relationship of composition and temperature is derived

$$X_j=\left(\alpha p e^{b/\left(T_j+c\right)-a}-1\right)/(\alpha-1) \tag{17}$$

where T_j is the temperature of stage j, p is the pressure of rectifying column or stripping column, α is the relative volatility. Then the composition in stage j can be derived from Eq. 17.

The simplified model system should track the output variables as accurately as possible when operating conditions change, which is an important criterion for evaluating model validity in control system design. In ITCDIC, we concentrate more attention on the track of the concentrations of the top and bottom stages because the ultimate target is to keep them consistent with the set-points.

Same as earlier, benzene-toluene system is taken as an illustration. The system is disturbed by a +20% step change of the feed flow F 0.3 h after the initial time. Figure 4 shows the changes of the liquid concentrations at the top and bottom stages calculated by the mechanism model,[7] the simplified wave model proposed above and the wave model presented in the literature.[46] From the figure, we can see that the three curves are too close to distinguish each other, so we depict the errors of the concentrations by the two wave models in Figure 5, respectively. From Figure 5, the advantages of this model exhibit in two aspects: smaller error and also faster speed in eliminating error. The error comes close to zero soon in the simplified wave model, which means that the error would not be accumulated and the wave model could self-tune.

The results prove our inference that the errors of stages 1 and n between the real concentration from the mechanism model and the concentration from the wave model could be further eliminated, which has been analyzed earlier.

Generalized Generic Model Controller Design for ITCDIC Based on Wave Model

Basic principle of Generalized Generic model control

Generalized generic model control (GGMC) was first proposed by Wang et al.,[47] which is an expansion coming from generic model control (GMC).[48] GGMC inherits the advantages of GMC, for example, nonlinear process model can be directly used, controller parameters can be easily tuned and model/plant mismatch can be compensated. Also, GGMC has its own advantages over GMC, for instance, GGMC can easily handle nonlinear MIMO processes with relative order larger than one, and furthermore, MIMO nonlinear processes can be naturally decoupled by GGMC.

Consider the following MIMO nonlinear process

$$\dot{x}(t)=f(x,d,\theta)+g(x,d,\theta)u(t) \tag{18}$$

$$y(t)=h(x) \tag{19}$$

where the state vector $x(t)\in R^n$, the input vector $u(t)\in R^m$, the output vector $y(t)\in R^m$, d is disturbance vector, θ is the process parameter vector, and f, g, h are nonlinear functions.

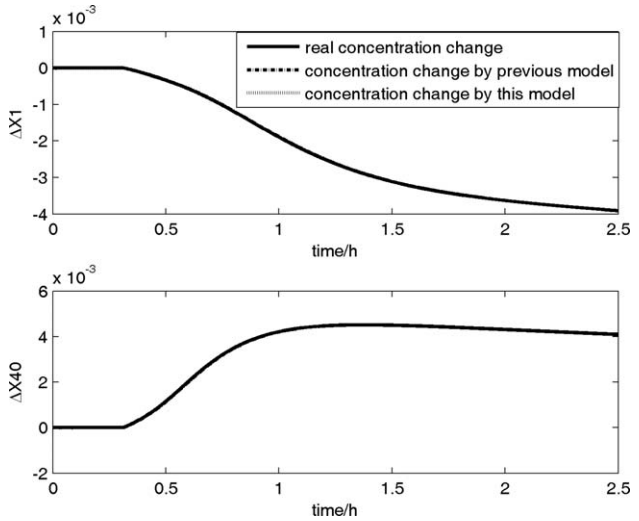

Figure 4. The liquid concentration of the two wave models and the mechanism model under +20% step disturbance of *F*.

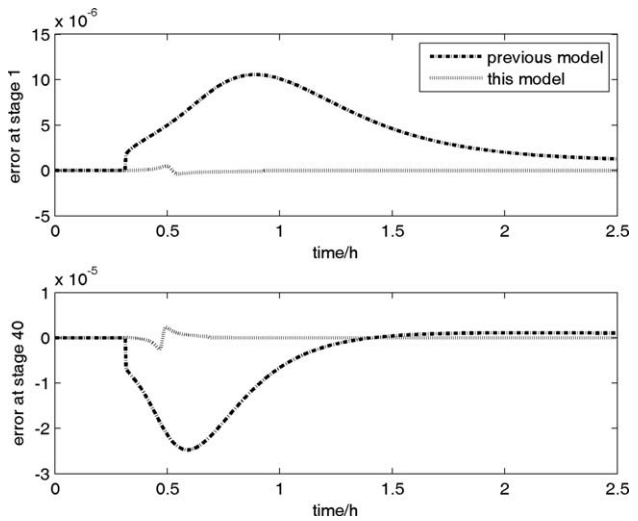

Figure 5. The errors between the wave models and the mechanism model under +20% step disturbance of *F*.

Assume that the relative orders of the system are $r=\{r_1,r_2,\ldots,\ r_{\mathrm{m}}\}$, and the reference trajectory for the ith process output y_i is as follows

$$y_i^{r_i}+k_{ir_i}y_i^{(r_i-1)}+\ldots+k_{i2}\dot{y}_i=k_{i1}\left(\dot{y}_i^*-\dot{y}_i\right)+k_{i0}\int_0^{t_n}\left(\dot{y}_i^*-\dot{y}_i\right)dt \quad (20)$$

where y_i is the output variable, $k_{ir_i},\ldots,k_{i0}$ are controller parameters, and y^* is the set-point.

Then the solving of u is transformed into the following optimal control problem:

$$\begin{aligned}\min_{u(t)}\quad & \int_0^{t_n}\left[H(x,u,d,t)^T W H(x,u,d,t)\right]dt\\ st.\quad & \dot{x}=f(x,d,\theta)+g(x,d,\theta)u(t)\\ & y=h(x)\end{aligned} \quad (21)$$

where W is a weighting matrix $H(x,u,d)=[h_1,h_2,\ldots,h_m]^T$ and

$$h_i=y_i^{r_i}+k_{ir_i}y_i^{(r_i-1)}+\ldots+k_{i2}\dot{y}_i-k_{i1}\left(\dot{y}_i^*-\dot{y}_i\right)-k_{i0}\int_0^{t_n}\left(\dot{y}_i^*-\dot{y}_i\right)dt \quad (22)$$

If there are no constraints, and at least one element of u appears in each of the m equations represented by 20, then u can be solved out. For details and the stability analysis of GGMC, see Wang et al.[45]

Generalized Generic model control for ITCDIC

In ITCDIC, the controlled variables are the concentrations of the top and bottom products, Y_1 and X_n, and the manipulated variables are the pressure of the rectifying section (P_{r}) and feed thermal condition (q). Because Y_1 can be easily derived from X_1 by vapor–liquid equilibrium relationships, for convenience, X_1 and X_{n} are controlled.

Normally, the derivative of the reference trajectory in a generic model control (GMC) for ITCDIC is of the following form

$$\dot{X}_i=k_{i1}(X_i{}^*-X_i)+k_{i2}\int_0^t(X_i{}^*-X_i)dt,\ i=1,n \quad (23)$$

Define

$$Kv_1=(X_{r\_\max}-X_{r\_\min})\frac{-k_r\exp(-k_r(1-S_1))}{(1+\exp(-k_r(1-S_1)))^2} \quad (24)$$

$$Kv_n=(X_{s\_\max}-X_{s\_\min})\frac{-k_s\exp(-k_s(n-S_2))}{(1+\exp(-k_s(n-S_2)))^2} \quad (25)$$

Then combining Eqs. 3 and 4, Eqs. 5 and 6 can be written as

$$\dot{X}_1=Kv_1\dot{S}_1 \quad (26)$$

$$\dot{X}_n=Kv_n\dot{S}_2 \quad (27)$$

Combining Eqs. 26 and 27 for briefness, we can obtain

$$\dot{X}_i=Kv_i\dot{S},\ i=1,n \quad (28)$$

where $\dot{S}$ represents $\dot{S}_1$ or $\dot{S}_2$. From Eq. 28 we can obtain the following equation

$$\ddot{S}=\frac{\ddot{X}_i}{Kv_i}-\frac{\dot{K}v_i\dot{X}_i}{Kv_i{}^2},\ i=1,n \quad (29)$$

The combination of Eqs. 23, 28 and 29 leads to

$$\ddot{S}=\frac{-k_{i1}\dot{X}_i+k_{i2}\left(X_i^*-X_i\right)}{Kv_i}-\frac{\dot{K}v_ik_{i1}\left(X_i^*-X_i\right)+\dot{K}v_ik_{i2}\int_0^t\left(X_i^*-X_i\right)dt}{Kv_i^2},\ i=1,n \quad (30)$$

Use 29 to substitute into 30 and we have

$$\ddot{X}_i+k'_{i2}\dot{X}_i=k'_{i1}\left(X_i^*-X_i\right)+k'_{i0}\int_0^t\left(X_i^*-X_i\right)dt,\ i=1,n \quad (31)$$

where

$$k'_{i2}=Kv_ik_{i1}-\dot{K}v_i \quad (32)$$

$$k'_{i1}=Kv_ik_{i2}-\dot{K}v_ik_{i1} \quad (33)$$

$$k'_{i0}=-\dot{K}v_ik_{i2} \quad (34)$$

From Eqs. 23 to 31, a conventional GMC controller of ITCDIC is converted to a GGMC controller based on the nonlinear wave model. Although there are 6 controller parameters (k'_{i0}, k'_{i1} and k'_{i2}) in 31, it is obvious that based on Eqs. 32–34 the values of the six parameters are determined by k_{i1},k_{i2}, which means that the transformation does not increase the number of the parameters. Furthermore, Kv_i in 24 and 25 is calculated online in the process and, hence, plays the role of self-tuning in GGMC, which is a huge advantage over traditional GMC. Also, it is worth noting that Kv_i contains the information of the profile shape and, hence, renders the self-tuning a physical meaning.

According to Eqs. 3, 4 and 16, we can obtain

$$\ddot{X}_1=\left(\dot{V}_2Y_2+V_2\dot{Y}_2-\dot{V}_1Y_1-V_1\dot{Y}_1-\dot{L}_1X_1-L_1\dot{X}_1\right)/H \quad (35)$$

$$\ddot{X}_n=\left(-\dot{V}_nY_n-V_n\dot{Y}_n+\dot{L}_{n-1}X_{n-1}+L_{n-1}\dot{X}_{n-1}-\dot{L}_nX_n-L_n\dot{X}_n\right)/H \quad (36)$$

$$\dot{Y}_1=\frac{\alpha\dot{X}_i}{[(\alpha-1)X_i+1]^2} \quad (37)$$

Transformations of Eqs. 10–15 lead to the following equations

$$\dot{V}_1=F(1-\dot{q}) \quad (38)$$

$$\dot{L}_1=\frac{\dot{Q}_1}{\lambda} \quad (39)$$

$$\dot{V}_2=\dot{V}_1+\dot{L}_1 \quad (40)$$

$$\dot{L}_n=F\dot{q} \quad (41)$$

$$\dot{V}_n=\frac{\dot{Q}_{n-f+1}}{\lambda} \quad (42)$$

$$\dot{L}_{n-1}=F\dot{q}+\dot{V}_n \quad (43)$$

The derivative form of Eq. 7 is

$$\dot{Q}_i=Kq_i\dot{P}_r+Bq_i \quad (44)$$

where

Table 2. Integral Absolute Value of Error (IAE) [10^{-6}]

Control strategy	WGGMC		WGMC		TGMC	
	Top	Bottom	Top	Bottom	Top	Bottom
Servo	6.183	5.224	11.98	11.56	27.29	20.68
$F+15\%$	0.1316	0.5216	0.2385	0.8388	51.38	5.916
$Z_f+15\%$	0.4484	3.042	2.740	3.558	12.01	9.925
$P_s+15\%$	0.1481	0.4858	0.7030	1.123	87.37	11.20

$$Kq_i = \frac{UA \cdot b}{\left(a - \ln P_{vp,i}\right)^2 \left(X_i + (1 - X_i)/\alpha\right)} \tag{45}$$

$$Bq_i = \frac{-UA \cdot b \cdot P_r (1 - 1/\alpha)\dot{X}_i}{\left(a - \ln P_{vp,i}\right)^2 \left(X_i + (1 - X_i)/\alpha\right)^2} + \frac{-UA \cdot b \cdot P_s (1 - 1/\alpha)\dot{X}_{i+f-1}}{\left(a - \ln P_{vp,i+f-1}\right)^2 \left(X_{i+f-1} + \left(1 - X_{i+f-1}\right)/\alpha\right)^2} \; i = 1, 2, \ldots, f-1 \tag{46}$$

Incorporating Eqs. 37–46 into Eqs. 35 and 36, and combining Eq. 31, we can obtain the analytical solutions of dq/dt and dPr/dt, which are the derivatives of the manipulated variables. With the aforementioned procedure the system is naturally decoupled by the GGMC controller.

Case Study

An ideal ITCDIC with 40 stages is chosen as a representative column where binary mixture, benzene-toluene is separated. Detailed initial operating conditions are shown in Table 1.

For the high-purity control of this ITCDIC, we adopted another two control strategies as comparisons with the proposed generalized generic model controller based on simplified nonlinear wave model (WGGMC): the GMC controller based on the traditional data-driven model (TGMC) and the WGMC controller proposed by Liu et al.[46] in the preceding research. Detailed comparisons show that our control strategy (WGGMC) outperforms the other two control strategies. Table 2 presents the integrated absolute errors (IAE). However, Figures 6–9 illustrate the efficiency of WGGMC.

In the very-high-purity control of ITCDIC, the set-point of the top increases to 0.99999. In this case, TGMC and WGMC fail to work properly, while WGGMC can handle it well. We also add some disturbances in the process and the WGGMC controller is qualified for the job as well. The specific performance can be seen from Figures 10–12.

The following section will describe the performances of different controllers in detail.

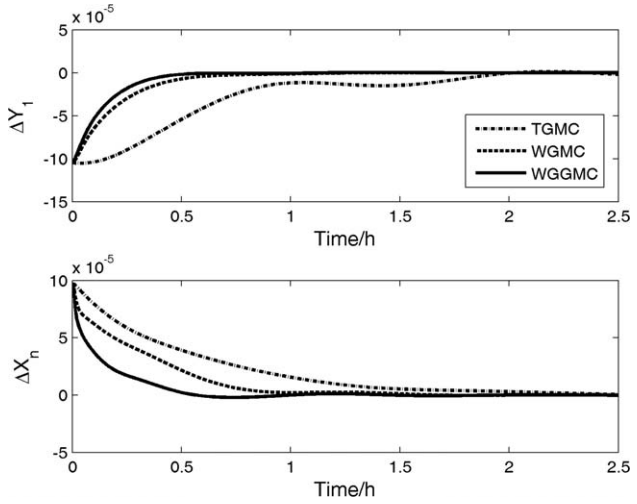

Figure 6. Servo control when set-points are set as 0.9991 and 0.0029.

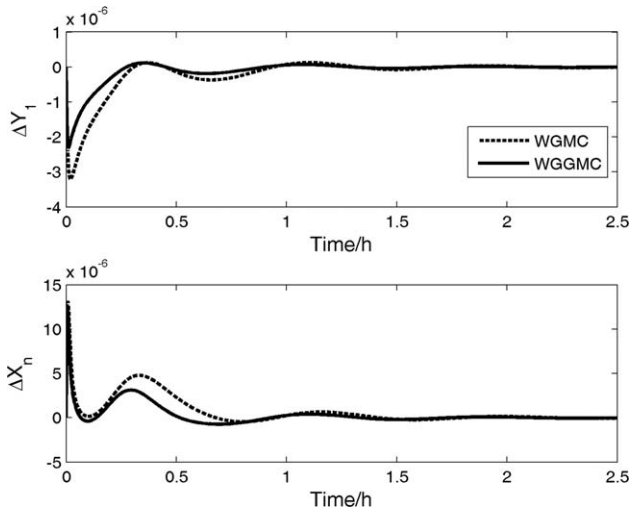

Figure 7. +15% step disturbance of *F*.

High-purity control

Servo Control. Figure 6 compares the servo control results of the three controllers when we change the top set-point from 0.998995 to 0.9991, and meanwhile change the bottom set-point from 0.002997 to 0.0029. It takes about 2 h for TGMC to reach new set-points in both top and bottom sections, and it takes about 1 h for WGMC to reach the new operating point. At the top end, the performance of WGGMC is a little better than that of WGMC; however, it only takes about 0.5 h for WGGMC to track the new set-point at the bottom, which is much better than WGMC. Altogether, TGMC has the most sluggish response speed, while WGGMC responses with the fastest speed.

Regulatory Control. The feed flow rate F, the feed mole fraction Z_f and the pressure of the stripping section P_s are the main disturbances for ITCDIC. When system stay at a

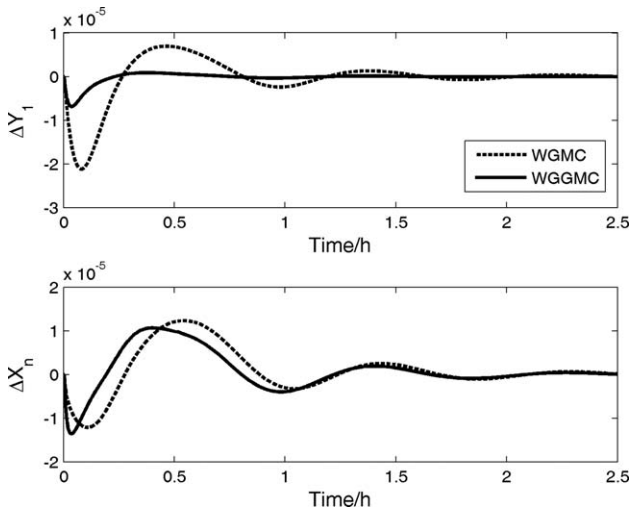

Figure 8. +15% step disturbance of Z_f.

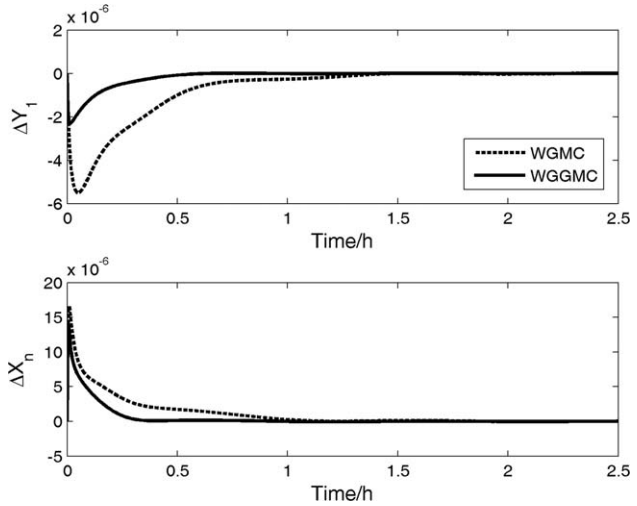

Figure 9. +15% step disturbance of P_s.

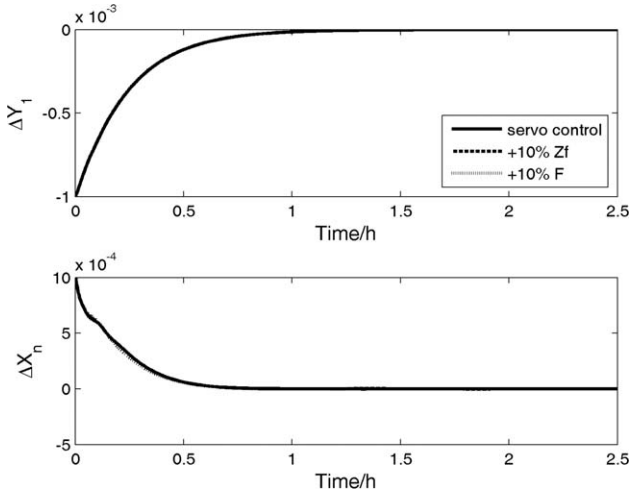

Figure 11. Very-high-purity control with disturbances.

steady operating point, step disturbances from F, Z_f and P_s are introduced into the system, respectively and the responses of the three controllers are investigated. Although TGMC could control the system, the deviation is rather large and the response is rather sluggish. The performances of TGMC are far from the other two controllers, and hence the responses of TGMC are not depicted in the figures so as to see clearly the comparison of WGGMC and WGMC.

Figure 7 shows the regulatory control of WGGMC and WGMC under a +15% step change of F. Both controllers handle the disturbance well. The transition time of the two responses is almost the same, but the oscillation of WGGMC is weaker than that of WGMC.

Figure 8 shows the comparison results of WGGMC and WGMC under a +15% step change of Z_f. From the figure, although the performances are almost well-matched in the control of the bottom product, WGMC shows a larger deviation and also the response is more sluggish in the control of the top product, taking about 1.5 h to be stable, whereas it takes only less than 0.5 h for WGGMC to return to the steady state.

Figure 9 presents the comparison of WGGMC and WGMC under a +15% step change of P_s. WGMC shows a large deviation in the control of the top product. It takes about 1.5 h for WGMC to return to the desired state, while WGGMC only needs 0.5 h at the top and the deviation at the top is very small. At the bottom, the advantages of WGGMC are also apparent.

Table 2 shows IAE of the different processes. It can be seen obviously that although WGMC has a larger improvement compared to TGMC, the errors of the WGGMC system are much smaller than that of WGMC at both ends of the column. The results reveal the efficiency of WGGMC in both servo control and regulatory control.

Very high-purity control

Figure 10 shows the performances of WGGMC in very-high-purity control. The top set-point increases from 0.998995 to 0.99999 and meanwhile the bottom set-point decreases from 0.002997 to 0.002. From the figure, WGGMC works well in the very-high-purity control. It takes about 1 h for the bottom to reach the new set-point. The

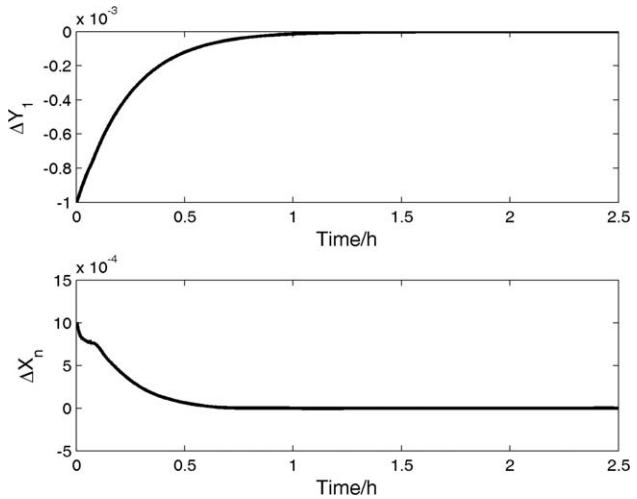

Figure 10. Servo control when set-points are set as 0.99999 and 0.002.

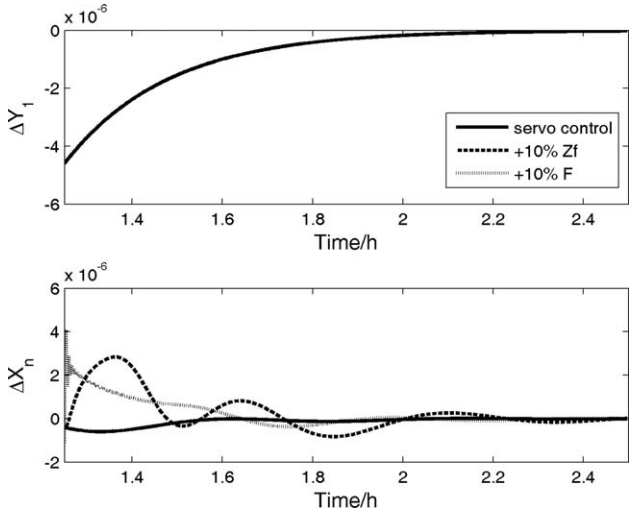

Figure 12. Partial enlarged figure of very-high-purity control with disturbances.

purity of the top increases a little slow because the purity is rather high and the offset is eliminated after 2 h.

In Figure 11, a +10% step change of F and a +10% step change of Z_f are also introduced, respectively 1.25 h after the initial time. Because the purity of the top product is very high, the performances of the controller after disturbances are introduced are difficult to be observed. So we enlarge Figure 11 from 1.25 h to 5 h in order to see clearly, as shown in Figure 12. The top product reaches an extremely high purity and the impact of the disturbances is too small to be observed from the figure, so the curves of the top end almost coincide. At the bottom, the impact is apparent. The disturbance of F is eliminated quickly, while the disturbance of Z_f leads to a little oscillation and it takes a longer time for the controller to eliminate the impact. Overall, WGGMC could handle the disturbances in very-high-purity ITCDIC.

Conclusion

In this work, a simplified nonlinear wave model of ITCDIC is established based on a nonlinear wave theory. The model test shows that the model has great accuracy especially at the top and bottom stages, which is very conducive to the control design. A generalized generic model control strategy based on this wave model (WGGMC) is then introduced into the system. WGGMC not only inherits the advantages of conventional GMC, but also realizes the self-tuning with a physical meaning. In the case study of the benzene-toluene ITCDIC system, compared with a GMC strategy based on a data-driven model and another wave-model-based GMC (WGMC), WGGMC has the best performance. In the very-high-purity control of ITCDIC, TGMC and WGMC fail to work properly, while WGGMC can handle it well even if there are disturbances. The whole work proves the efficiency of the presented wave model and the control system of ITCDIC.

Acknowledgments

This work is supported by Joint Funds of NSFC-CNPC of China (Grant U1162130), National High Technology Research and Development Program (863, Grant 2006AA05Z226), Zhejiang Provincial Natural Science Foundation for Distinguished Young Scientists (Grant R4100133) and Scholarship Award for Excellent Doctoral Student granted by Ministry of Education, and their supports are thereby acknowledged.

Notation

a,b,c = coefficient of the Antoine equation
F = feed flow rate, kmol h^{-1}
H = stage holdup, kmol
k_r,k_s = characterize the tangent of the inflection points S_1 and S_2
L = liquid flow rate, kmol h^{-1}
Pr = pressure of rectifying section, Mpa
Ps = pressure of stripping section, Mpa
P_{vp} = vapor saturated pressure, Mpa
Q = energy required, kW
q = feed thermal condition
R = the desired value of the controlled variables
S_1 = inflection point of rectifying section
S_2 = inflection point of stripping section
T = absolute temperature, K
UA = heat-transfer rate, W K^{-1}
V = vapor flow rate, kmol h^{-1}
X = mole fraction of liquid
X_{r_min} = the minimum asymptotic limits of the rectifying section
X_{r_max} = the maximum asymptotic limits of the rectifying section
X_{s_min} = the minimum asymptotic limits in the stripping section
X_{s_max} = the maximum asymptotic limits in the stripping section
$\bar{X}$ = the estimation of liquid mole fraction
Y = mole fraction of vapor
Z_f = mole fraction of feed

Greek letters

α = relative volatility
λ = latent heat, J $kmol^{-1}$

Subscripts

f = feed stage
j = stage number (counted from the top to the bottom, namely, from 1 to n)
r = the rectifying section
s = the stripping section

Literature Cited

1. Jana AK, Mane A. Heat pump assisted reactive distillation: wide boiling mixture. *AIChE J*. 2011;57:3233–3237.
2. Olanrewaju MJ, Huang B, Afacan A. Development of a simultaneous continuum and noncontinuum state estimator with application on a distillation process. *AIChE J*. 2012;58:480–492.
3. Lu S, Lei Z, Wu J, Yang B. Dynamic control analysis for manufacturing ethanol fuel via reactive distillation. *Chem Eng Process*. 2011;50:1128–1136.
4. Liu W, Huang K, Zhang L, Chen H, Wang S-J. Dynamics and control of totally refluxed reactive distillation columns. *J Process Contr*. 2012;22:1182–1197.
5. Mah RSH, Nicholas JJ, Wodnik RB. Distillation with secondary reflux and vaporization: a comparative evaluation. *AIChE J*. 1977; 23:651–658.
6. Takamatsu T, Nakaiwa M, Huang K, Akiya T, Noda H, Nakanishi T, Aso K. Simulation oriented development of a new heat integrated distillation column and its characteristics for energy saving. *Comput Chem Eng*. 1997;21:S243–S247.
7. Liu XG, Qian JX. Modeling, control, and optimization of ideal internal thermally coupled distillation columns. *Chem Eng Technol*. 2000;23:235–241.
8. Kiss AA. Heat-integrated reactive distillation process for synthesis of fatty esters. *Fuel Process Technol*. 2011;92:1288–1296.
9. Lin Q, Liu G, Huang K, Wang S, Chen H. Balancing design and control of an olefin metathesis reactive distillation column through reactive section distribution. *Chem Eng Sci*. 2011;66:3049–3055.
10. Jiao Y, Wang S-J, Huang K, Chen H, Liu W. Design and analysis of internally heat-integrated reactive distillation processes. *Ind Eng Chem Res*. 2012;51:4002–4016.
11. Kim YH. Approximate design and cost evaluation of internally heat-integrated distillation columns (HIDiCs). *Kor J Chem Eng*. 2012;29: 1004–1009.
12. Chang L, Liu X, Dai L, Sun Y. Modeling, characteristic analysis, and optimization of ideal internal thermally coupled air separation columns. *Ind Eng Chem Res*. 2012;51:14517–14524.
13. Cabrera-Ruiz J, Jiménez-Gutiérrez A, Segovia-Hernández JG, Assessment of the implementation of heat-integrated distillation columns for the separation of ternary mixtures. *Ind Eng Chem Res*. 2011;50:2176–2181.
14. Nakaiwa M, Huang K, Owa M, Akiya T, Nakane T, Sato M, Takamatsu T. Energy savings in heat-integrated distillation columns. *Energy*. 1997;22:621–625.
15. Nakaiwa M, Huang K, Owa M, Akiya T, Nakane T, Takamatsu T. Operating an ideal heat integrated distillation column with different control algorithms. *Comput Chem Eng*. 1998;22:S389–S393.
16. Wang SJ, Huang HP, Yu CC. Design and control of a heat-integrated reactive distillation process to produce methanol and n-butyl acetate. *Ind Eng Chem Res*. 2011;50:1321–1329.
17. Huang K, Zhu F, Ding W, Wang S-J. Control of a high-purity ethylene glycol reactive distillation column with insights of process dynamics. *AIChE J*. 2009;55:2106–2121.
18. Olanrewaju MJ, Huang B, Afacan A. Online composition estimation and experiment validation of distillation processes with switching dynamics. *Chem Eng Sci*. 2010;65:1597–1608.

19. Li J, Xiao J, Huang Y, Lou HH. Integrated process and product analysis: A multiscale approach to paint spray. *AIChE J*. 2007;53: 2841–2857.
20. Xiao J, Huang Y, Qian Y, Lou HH. Integrated product and process control of single-input-single-output systems. *AIChE J*. 2007;53:891–901.
21. Zhu Y, Liu XG. Dynamics and control of high purity heat integrated distillation columns. *Ind Eng Chem Res*. 2005;44:8806–8814.
22. Zhu Y, Liu XG. Investigating control schemes for an ideal thermally coupled distillation column (ITCDIC). *Chem Eng Technol*. 2005;28: 1048–1055.
23. Zhu GY, Henson MA, Megan L. Dynamic modeling and linear model predictive control of gas pipeline networks. *J Process Contr*. 2001;11:129–148.
24. Liu XG, Wang CY, Cong L. Adaptive robust generic model control of high-purity internal thermally coupled distillation column. *Chem Eng Technol*. 2011;34:111–118.
25. Liu XG, Wang CY, Cong L, Ding F. Adaptive generalized predictive control of high purity internal thermally coupled distillation column. *Can J Chem Eng*. 2012;90:420–428.
26. Jana AK. Heat integrated distillation operation. *Appl Energy*. 2010; 87:1477–1494.
27. Epple U, Gilles ED, Marquardt W. Model reduction for systems with wave propagation. *Chem Eng Tech*. 1987;59:611–612.
28. Marquardt W. Traveling waves in chemical processes. *Int Chem Eng*.1990;30:585–606.
29. Helfferich FG, Whitley RD. Non-linear waves in chromatography II. Wave interference and coherence in multicomponent. *J Chromatogr A*. 1996;734:7–47.
30. Marquardt W. Nichtlineare Wellenausbreitung - Ein Weg zu reduzierten dynamischen Modellen von Stofftrennprozessen. PhD Thesis. VDI-Fortschrittsberichte, Reihe 8, Nr. 161, VDI-Verlag, Düsseldorf, 1988.
31. Hwang YL, Helfferich FG. Nonlinear waves and asymmetric dynamics of countercurrent separation processes. *AIChE J*. 1989;35:690–693.
32. Hwang YL. On the nonlinear wave theory for dynamics of binary distillation columns. *AIChE J*. 1995;41:190–194.
33. Hwang YL. Nonlinear wave theory for dynamics of binary distillation columns. *AIChE J*. 1991;37:705–723.
34. Marquardt W, Amrhein M. Development of a linear distillation model from design data for process control. *Comput Chem Eng*. 1994;18:S349–S353.
35. Kienle A. Low-order dynamic models for ideal multicomponent distillation processes using nonlinear wave propagation theory. *Chem Eng Sci*. 2000;55:1817–1828.
36. Balasubramhanya LS, Doyle FJ. Nonlinear control of a high-purity distillation column using a traveling-wave model. *AIChE J*. 1997;43: 703–714.
37. Luyben WL, Control of distillation columns with sharp temperature profiles. *AIChE J*. 1971;17:713–718.
38. Luyben WL, Profile position control of distillation columns with sharp temperature profiles. *AIChE J*. 1972;18:238–240.
39. Han M, Park S. Control of high-purity distillation column using a nonlinear wave theory. *AIChE J*. 1993;39:787–796.
40. Zhu GY, Henson MA, Megan L. Low-order dynamic modeling of cryogenic distillation columns based on nonlinear wave phenomenon. *Sep Purif Technol*. 2001;24:467–487.
41. Bian SJ, Henson MA, Belanger P, Megan L. Nonlinear state estimation and model predictive control of nitrogen purification columns. *Ind Eng Chem Res*. 2005;44:153–167.
42. Bian SJ, Henson MA. Measurement selection for on-line estimation of nonlinear wave models for high purity distillation columns. *Chem Eng Sci*. 2006;61:3210–3222.
43. Stein E, Kienle A, Gilles ED. Dynamic optimization of multicomponent distillation processes. In: Keil F, Mackens W, Vo ßH, Werther J. Scientific Computing in Chemical Engineering II. Berlin: Springer; 1999:362–369.
44. Hankins NP. A non-linear wave model with variable molar flows for dynamic behaviour and disturbance propagation in distillation columns. *Chem Eng Res Des*. 2007;85:65–73.
45. Liu XG, Zhou YX, Cong L, Zhang J. Nonlinear wave modeling and dynamic analysis of internal thermally coupled distillation columns. *AIChE J*. 2012;58:1146–1156.
46. Liu XG, Zhou YX, Cong L, Ding F. High-purity control of internal thermally coupled distillation columns based on nonlinear wave model. *J Process Contr*. 2011;21:920–926.
47. Wang D, Zhou DH, Jin YH, Morse AS. Adaptive generalized generic model control and stability analysis. *Comput Chem Eng*. 2003;27:1617–1629.
48. Lee PL, Sullivan GR. Generic model control (GMC). *Comput Chem Eng*. 1988;12:573–580.

Manuscript received Dec. 18, 2012, and revision received Mar. 20, 2013.